

SIMILARITY IN THE BEHAVIOUR OF INITIALLY SATURATED OR SUBCOOLED LIQUID JETS DISCHARGING THROUGH A NOZZLE

H. CHAVES, T.A. KOWALEWSKI, T. KURSCHAT, G.E.A. MEIER and E.A. MÜLLER

Max-Planck-Institut für Strömungsforschung, P.O. Box 867, D-3400 Göttingen, FRG

Received 16 June 1988

The discharge of high-temperature, high-pressure liquid from a nozzle into a low-pressure environment results in a quick transition from subcooled to a superheated state of the liquid. When finally the liquid reaches an ambient pressure P_c , which is far below its saturation pressure P_s , it evaporates steadily or flashes explosively into vapour. The influence of specific heat of the fluid and of the initial temperature on this process is the subject of the present investigation. Using a differential interferometer the amount of vapour present in the jet was evaluated qualitatively. The initial jet angles were measured. These experimental results are compared with the results obtained from a homogeneous equilibrium model for isentropic expansion of the two-phase jet. On exit from the nozzle a superheated liquid state was assumed in order to calculate jet angles. The substances investigated were perfluoro-*n*-hexane, perfluoro-1,3-dimethylcyclohexane, ethanol and water.

1. Introduction

Much effort has been put into the study of atomizing jets, mainly because of their application in fuel injection. Most of the experimental work is done under conditions, where the liquid is not likely to evaporate. The theoretical interpretation of the results is based on mechanical or aerodynamic instabilities of the jet. However, if the exit pressure of the jet is below the saturation pressure of the liquid, evaporation comes to play an important role. Its effect can be much stronger than the disintegration effects caused by mechanical or aerodynamic forces. How large the effect of evaporation on a jet is, depends on the energy balance between internal energy of the fluid available for evaporation and its heat of evaporation. For fluids with a high molar specific heat the internal energy present in the hot liquid can be much larger than the heat of vaporization. Under certain adiabatic conditions such liquids can evaporate completely or the vapour can liquefy completely (retrograde behaviour). Figs. 1a and 1b show temperature-entropy diagrams for substances with low and high molar specific heat. The limit between "normal" and "retrograde" substances is reached when the vapour saturation boundary becomes per-

pendicular in the temperature-entropy diagram. It can be seen that at higher initial temperatures (arrow in fig. 1) it is possible to fully evaporate a "retrograde" fluid adiabatically, while a liquid with low molar specific heat can only be evaporated partially. However, as the specific heat of a substance is not constant and depends on temperature, the ideal-gas molar specific heat for constant volume at the critical temperature $C_v^0(T_c)/R$ is chosen as a characteristic value for each substance. The value of the characteristic molar specific heat necessary for retrograde behaviour is 12 gas constants [1]. Retrograde behaviour of fluids with high molar specific heat has been studied in previous shock-tube experiments [1,2].

2. Experimental

2.1. Apparatus and measuring procedures

In the experiments the liquid was discharged during a short opening time (≈ 10 ms) of an electrically driven automotive injection nozzle of ≈ 1 mm outer orifice diameter. The nozzle is heated with the help of electrical foils. The temperature was regulated with a tolerance of 0.3°C . The test substance was pressur-

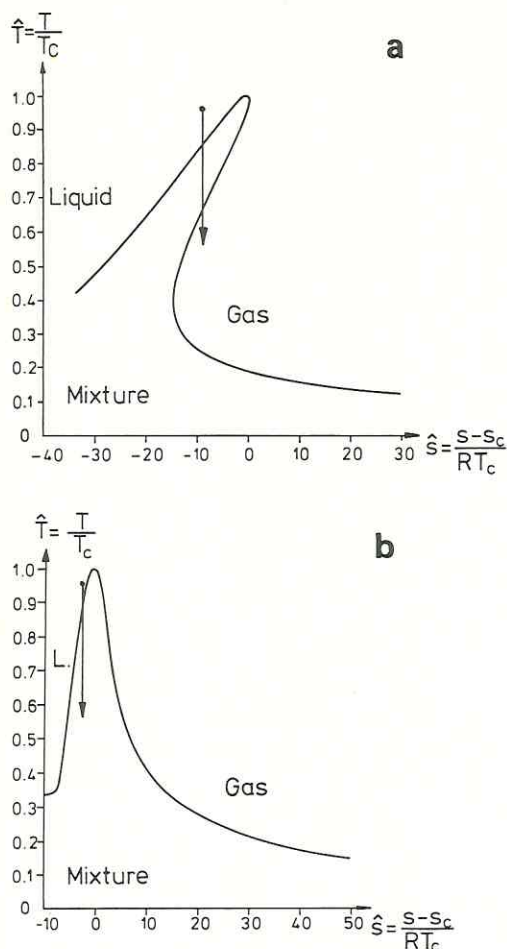


Fig. 1. (a) Temperature-entropy diagram for a substance of high molar specific heat with the saturation boundary; the arrow indicates an isentropic expansion from a liquid state to a pure vapour state. (b) Temperature-entropy diagram for a substance of low molar specific heat with the saturation boundary; the arrow shows that for isentropic expansion of a liquid the end state will always be a two-phase mixture.

ized within a bellows surrounded by nitrogen under pressure. This helped to avoid gases being dissolved into the test liquid. A specially constructed light-emitting-diode (LED) pulse generator [3] was used to obtain short illumination times (1–10 μ s) of the jet. A TV camera and a videoprinter were applied to register the jet images. The optical setup is shown in fig. 2. Using shadowgraph techniques and a differential interferometer, it was possible to distinguish

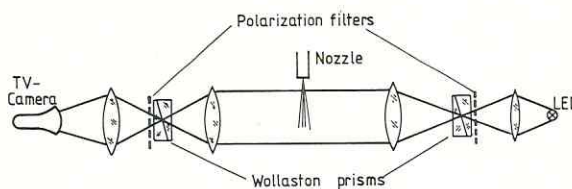


Fig. 2. Optical setup of the differential interferometer.

between two-phase and vapour regions of the jet.

Pictures of the jet were taken at initial temperatures in the range from 20 to 170°C and at initial pressures up to 1.1 MPa. The main aim of the experiments was to investigate the discharge of substances of varying specific heat, in this case PP1 (perfluoro-*n*-hexane), ethanol and water. A few experiments were performed with another retrograde substance PP3 (perfluoro-1,3-dimethylcyclohexane). The reasons for the choice of fully fluorinated hydrocarbons are of practical nature. First they are not inflammable and second they have much lower critical temperatures than the corresponding hydrocarbons (retrograde behaviour appears only at high temperatures – i.e. approximately greater than 0.7 times the critical temperature, see fig. 1).

2.2. Experimental results

Fig. 3a shows a differential interferogram of a water jet at an initial temperature of $T_0 = 120^\circ\text{C}$, fig. 3b, of an ethanol jet ($T_0 = 112^\circ\text{C}$) and fig. 3c, of a PP1 jet ($T_0 = 112^\circ\text{C}$). For all these experiments the reservoir pressure was $P_0 = 0.97$ Mpa. The jets were injected into atmospheric conditions, i.e. external pressure $P_e = 10^5$ Pa. The characteristic value of the molar specific heat C_p^0/R for water is 3.47 gas constants, for ethanol it is 11.47 and for PP1 it is 39.3 gas constants. The dark parts of interferograms represent the highly light absorbent two-phase part of the jet. The transparent vapour part of the jet is characterized by the interference fringes. In spite of the fact, that the boiling temperatures of water ($T_b = 100^\circ\text{C}$) and ethanol ($T_b = 78^\circ\text{C}$) are lower than the initial liquid temperature, the jets of water or ethanol show no marked difference in the large temperature range observed, and for both substances a large amount of liquid in the form of droplets is still present in the jet. The reason for this behaviour is that during adiabatic

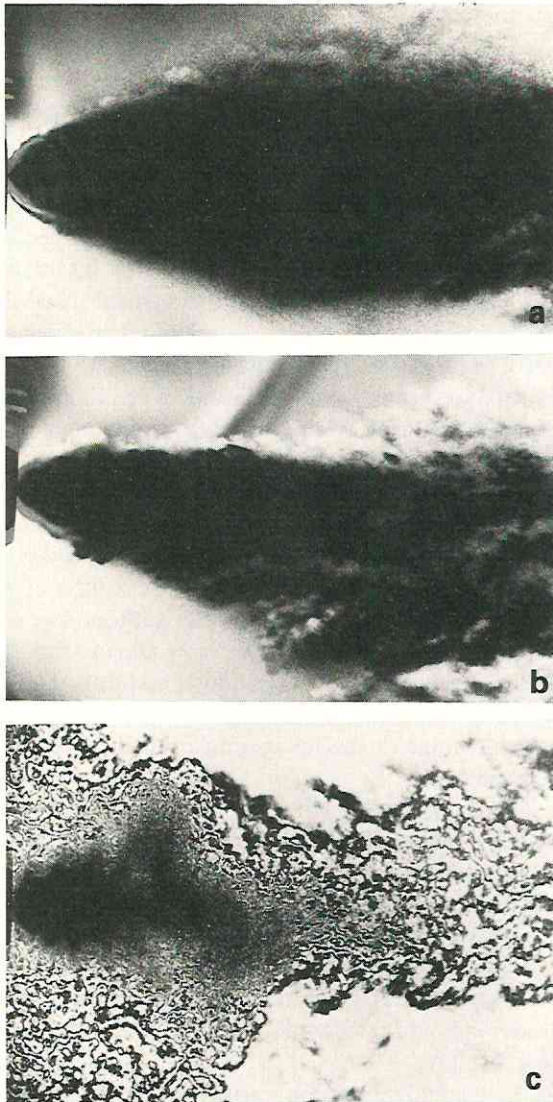


Fig. 3. (a) Superheated jet of water emerging into the atmosphere, initial pressure $P_0=0.97$ MPa, initial temperature 120°C , the reduced molar specific heat for constant volume at the critical temperature for water is $C_v^0(T_c)/R=3.47$. (b) Superheated jet of ethanol emerging into the atmosphere, initial pressure $P_0=0.97$ MPa, initial temperature 112°C , the reduced molar specific heat for constant volume at the critical temperature for ethanol is $C_v^0(T_c)/R=11.47$. (c) Superheated jet of perfluoro-*n*-hexane (PP1) emerging into the atmosphere, initial pressure $P_0=0.97$ MPa, initial temperature 112°C , the reduced molar specific heat for constant volume at the critical temperature for PP1 is $C_v^0(T_c)/R=39.3$.

evaporation outside of the nozzle, the liquid cools down very quickly to a temperature lower than the saturation temperature $T_s(P_e)$. In the case of a substance of high molar specific heat (PP1) the jet also cools down adiabatically. However, the amount of internal energy stored in the molecules is much larger than the latent heat of evaporation and only a small part of the internal energy is lost due to the evaporation process. In fig. 3c it can be seen that the PP1 jet evaporates completely at a distance 25 nozzle diameters downstream.

The main point of the present observations is the jet geometry. It was described by the following three parameters evaluated from the video images of the jet: the initial angle of expansion α , i.e. the angle of aperture of the jet immediately at the nozzle exit (fig. 4), the volume of the two-phase region of the jet V_z and the volume of the vapour region V_d (fig. 5). The volume of the vapour V_d and the two-phase parts V_z of the jet were calculated assuming axial symmetry of the jet. These volumes were normalized with the volume of a jet with no expansion V_0 (stable liquid jet). The calculations were limited to a distance of 6 mm from the nozzle. The abscissae of figs. 4 and 5 are a normalized temperature which has a value of zero

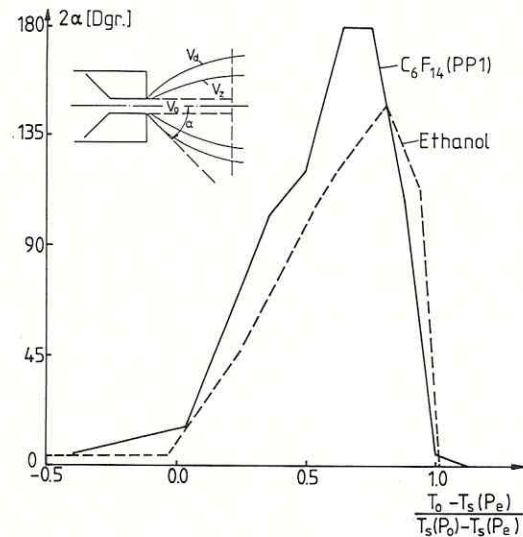


Fig. 4. Measured initial jet angle α versus relative superheat for ethanol and perfluoro-*n*-hexane, T_0 is the initial liquid temperature, $T_s(P_e)$ is the saturation temperature corresponding to the end pressure and $T_s(P_0)$ is the saturation temperature corresponding to the initial pressure.

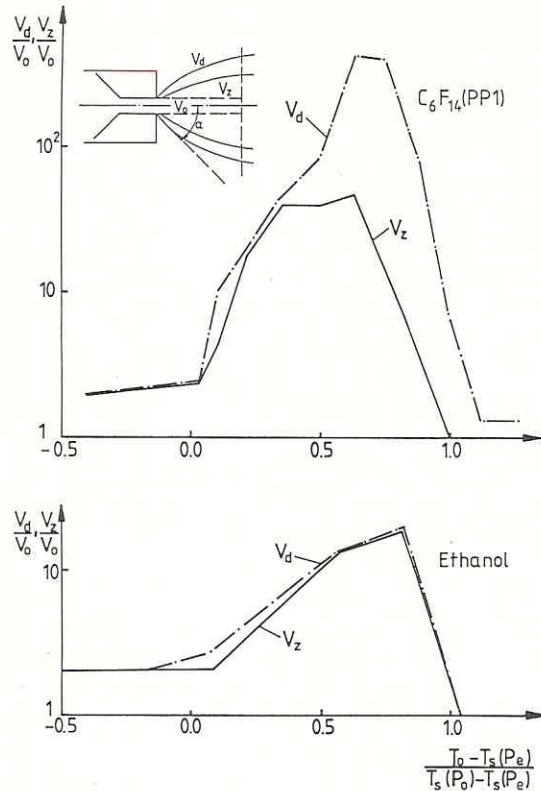


Fig. 5. Measured relative volumes of vapour V_d/V_0 and two-phase mixture V_z/V_0 over relative superheat for perfluoro-*n*-hexane (PP1) and ethanol, V_0 is the reference volume of the jet without expansion, T_0 is the initial liquid temperature, $T_s(P_e)$ is the saturation temperature corresponding to the end pressure and $T_s(P_0)$ is the saturation temperature corresponding to the initial pressure.

when the initial temperature T_0 is equal to the saturation temperature for the external pressure $T_s(P_e)$ and has a value of one when the initial temperature is equal to the saturation temperature for the given initial pressure $T_s(P_0)$. In other words, below zero of the so normalized temperature no evaporation occurs, above one, boiling of the liquid has to occur in the nozzle.

Fig. 4 shows clearly that the measured jet angles increase sharply with increasing degree of superheat and reach values which are limited in some cases only by the geometry of the experimental setup and not by the dynamics of the jet. The maximal jet angle is 180° since the nozzle hole is part of the injector tip, which is flat. In the range of temperatures used, the changes of the parameters typical of mechanical theories of

jet atomization like viscosity, surface tension or density cannot explain this change in the jet angle.

Four regimes of the jet phenomena can be distinguished. In the first one, at high subcooling of the liquid in the nozzle (negative normalized temperature, figs. 4 and 5), the jet angle α is small and evaporation is not present. At low Reynolds and Weber numbers the jet near the nozzle exit looks like a liquid cylinder of the diameter of the nozzle hole. With increasing exit velocity from the nozzle, mechanical instabilities begin to disturb the jet. At relatively low velocities it is caused by surface tension acting on the jet, which makes the cylinder of liquid an unstable figure of equilibrium (Rayleigh instability). At higher jet velocities also friction of the surrounding gas working on the jet surface causes a disruption of the jet surface (aerodynamic instability). The appearance of components of these forces perpendicular to the jet surface causes its disintegration. This regime of jet stability has been studied by many authors, e.g. ref. [4]. In the presence of evaporation, the mechanical disruption of the jet can become a second-order effect, and one can assume that a velocity component perpendicular to the jet issuing from the nozzle is negligible.

This second regime of jet instability is observed at positive, but small normalized temperatures. The jet consists of a liquid–vapour mixture, which creates a typical “bell” structure with relatively well defined boundaries. The angle of expansion α and volume V_z depend on the value of normalized temperature (superheat). In this regime the difference between retrograde and non-retrograde substances is very small (e.g. fig. 3a).

The dependence of the initial jet angle on normalized temperature can be described qualitatively in the following way. The superheated liquid emerging from the nozzle contains a large number of bubbles formed by nucleation. These bubbles are very small and their number increases exponentially with increasing superheat. Although the mass fraction of liquid evaporated is very small, because of the low gas density, the void fraction of the two-phase mixture increases rapidly. This causes a global expansion of the jet, and therefore an increase of the jet angle. Even for the case when vapour bubbles are already present in the liquid within the nozzle, they are not in mechanical equilibrium with the ambient pressure and they grow

very quickly expanding the jet. A void fraction of 0.5 is reached almost immediately after the exit from the nozzle, so that the two-phase flow changes from liquid–bubble to vapour–droplet flow. The global behaviour of the initial jet angle as a function of initial temperature (fig. 4) is not much different for all the substances used. Only a small amount of evaporation is needed to initially accelerate the droplets in the jet perpendicular to the nozzle axis. This is always possible even for fluids with a low specific heat.

In the third regime of jet behaviour, observed at higher superheat values (normalized temperatures of about 0.7) the difference between retrograde and non-retrograde substances becomes apparent in the volumes of vapour in the jet. In the case of retrograde substances jet evaporation has an explosive character, which completely disturbs the typical “bell shape” structure of the jet (fig. 3c). At normalized temperatures close to one the fluid starts to evaporate within the nozzle. Especially when the value of the initial temperature is above 0.9 that of the critical temperature of the fluid, nucleation has to occur within the nozzle, because for reduced temperatures greater than 0.9 the liquid spinodal limit is at positive pressures and can be easily attained within the nozzle if the external pressure is low. Most likely nucleation would be homogeneous in these cases, because for a given pressure drop in the nozzle the attainable superheat is much greater than for low temperatures. The resulting number of nuclei formed by homogeneous nucleation is much larger than the possible number of heterogeneous nuclei likely present in the liquid. In these cases the fluid issuing from the nozzle is a liquid–vapour mixture (especially for long nozzles) and therefore its effective value of superheat is smaller than assumed when the evaporation begins outside of the nozzle. It appears as a decrease of jet angle with increasing temperature observed for normalized temperature values above 0.7.

At values of normalized temperature greater than one a supersonic gas (vapour) jet is observed. This is the fourth regime of jet phenomena, which is well known in gasdynamics.

3. Theoretical background

With help of a simple thermodynamical model the jet angles (fig. 6) and the evaporated mass fraction

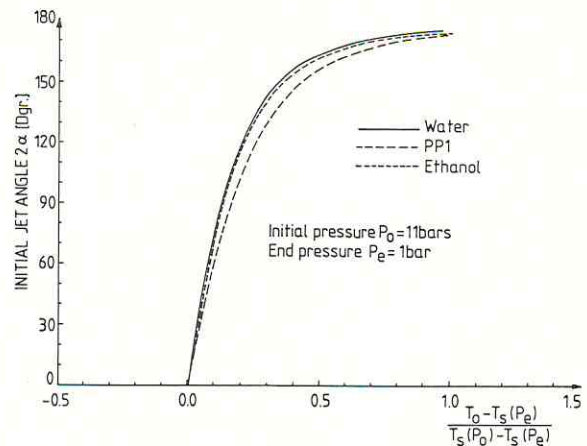


Fig. 6. Calculated initial jet angle α versus relative superheat, assuming that the fluid on exit of the nozzle is a superheated liquid, and that the end state of the isentropic non-mixing jet expansion is homogeneous and in thermal equilibrium.

were calculated (fig. 7). This model bases on a direct interpretation of the initial jet angle α as a ratio of the jet expansion velocity u_t (due to evaporation from a superheated liquid state) to the jet exit velocity u_f . Since these velocities are perpendicular one can derive α in the following way:

$$\tan \alpha = u_t / u_f. \quad (1)$$

The velocities u_f and u_t are calculated from the energy equations:

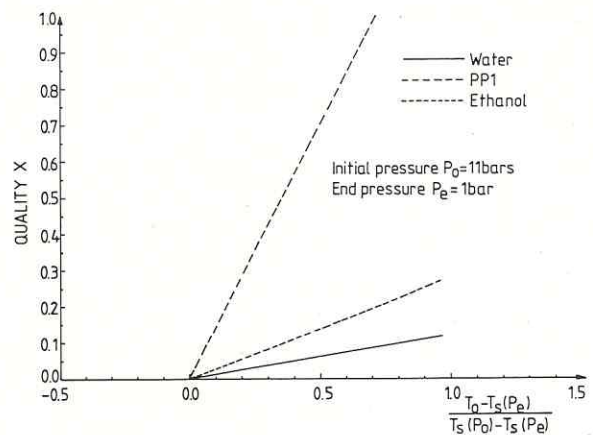


Fig. 7. Calculated mass fraction of vapour x (quality) in the jet after full expansion versus relative superheat for water, ethanol and perfluoro-*n*-hexane (PP1), using the same model as for fig. 6.

$$h_0 = h_{\text{sup}} + u_f^2/2, \quad (2)$$

$$h_{\text{sup}} = h_e + u_i^2/2, \quad (3)$$

where

$$h_e = xh_v + (1-x)h_l. \quad (4)$$

Here h_0 is the reservoir specific enthalpy, h_{sup} is the enthalpy of the superheated liquid emerging from the nozzle, and h_e is the enthalpy of the two-phase mixture at end state after the expansion and the evaporation of the jet took place, h_v is the specific enthalpy of the vapour, h_l the specific enthalpy of the liquid within the jet, and x is the mass fraction of vapour. The model assumes that at the end state the jet reaches an equilibrium as a homogeneous two-phase mixture and that the process is isentropic. This means that

$$s_e = s_0 = xs_v + (1-x)s_l, \quad (5)$$

where the subscript e means end state, 0 reservoir state and v, l vapour and liquid respectively.

Using the initial pressure P_0 and the initial temperature T_0 as independent variables and keeping the end or back pressure P_e constant, eq. (5) can be modified to show the effect of the specific heat on the global expansion process. The initial entropy s_0 is then a function of the two independent variables. For constant initial pressure P_0 , eq. (5) can be differentiated with respect to the initial temperature T_0 . The resulting equation for the change of quality x of the two-phase mixture with respect to the initial temperature is

$$\left. \frac{\partial x}{\partial T_0} \right|_{P_0} = \left. \frac{\partial s_0}{\partial T_0} \right|_{P_0} \frac{1}{s_v - s_l} = \frac{C_{p0}}{T_0} \frac{1}{s_v - s_l}. \quad (6)$$

The specific heat for constant pressure C_p of liquids depends only weakly on temperature and as long as the temperature range of the initial temperatures is not too large, this specific heat can be assumed constant. The evaporation entropy $s_v - s_l$ is constant for a given end state. These are the reasons why the quality curves in fig. 6 are almost straight lines.

Integrating eq. (6) one obtains

$$x = \frac{C_{p0}}{s_v - s_l} \ln \frac{T_0}{T_e}. \quad (7)$$

Since $0 \leq (T_0 - T_e)/T_e < 1$, then by expansion of the

logarithm and using the Clausius–Clayperon equations one gets

$$\begin{aligned} x &= \frac{C_{p0}}{s_v - s_l} \ln \left(1 + \frac{T_0 - T_e}{T_e} \right) \\ &\approx \frac{C_{p0}}{h_v - h_l} (T_0 - T_e). \end{aligned} \quad (8)$$

Eq. (8) shows that the mass fraction of vapour in the jet is directly proportional to the specific heat of the liquid and to the temperature difference between initial and end state. The temperature of the end state is the saturation temperature corresponding to the end or back pressure. The latent heat of evaporation $h_v - h_l$ is a function of the end temperature, or indirectly of back pressure. At the critical point, the latent heat is zero and increases with decreasing temperature. At low temperature levels (cryogenic) therefore no complete evaporation is possible because the specific heat of a substance decreases with temperature. Eq. (8) shows clearly the balance between internal energy and the heat of evaporation, although its range of usefulness is limited by the assumptions used to obtain it.

4. Summary and conclusions

The theoretical results are only qualitatively comparable with the experimental curves in figs. 4 and 5, although they show that the basic physics of the problem of superheated jets can be described with the help of such an initially superheated liquid, which isentropically expands to a final homogeneous equilibrium mixture. The effect of an increased molar specific heat of the fluid on the jet is small for the initial jet angle, but very strong for the amount of liquid evaporated. The initial jet angle depends basically only on the initial degree of superheat of the liquid. This is given by the initial temperature and the end or back pressure for the jet. The jet angles attained by superheating the liquid are an order of magnitude larger than could be explained by mechanical instabilities of the jet. In a first estimate the quality of the two-phase mixture after expansion in the jet is linear with the specific heat of the fluid and with the difference between initial and end temperature (given by the end pressure). In reality the flow

within the nozzle is viscous (non-isentropic), the jet mixes with the surrounding gas, the droplets and the vapour separate (non-homogeneous, fig. 3c) and thermodynamic equilibrium is only attained after a much longer period of time as assumed in the model. These phenomena are the basis for further detailed work.

References

- [1] G. Detleff, P.A. Thompson, G.E.A. Meier and H.D. Speckmann, *J. Fluid Mech.* 95 (1979) 279.
- [2] P.A. Thompson, H. Chaves, G.E.A. Meier, Y.G. Kim and H.D. Speckmann, *J. Fluid Mech.* 185 (1987) 385.
- [3] W.J. Hiller, H.M. Lent, G.E.A. Meier and B. Stasicki, *Exp. Fluids* 5 (1987) 141.
- [4] R.D. Reitz and F.V. Bracco, *Phys. Fluids* 25 (1982) 1730.

